Lithuanian Journal of Physics, Vol. **47**, No. 4, pp. 403–410 (2007)

EFFICIENT FOUR-WAVE PARAMETRIC AMPLIFICATION AND SPATIAL SOLITON GENERATION IN TRANSPARENT ISOTROPIC MEDIUM WITH KERR NONLINEARITY *

H. Valtna [a,b], A. Dubietis [a], G. Tamošauskas [a], P. Polesana [a,c], J. Galinis [a], D. Majus [a], G. Valiulis [a], D. Faccio [c], P. Di Trapani [a], and A. Piskarskas [a]

[a] *Department of Quantum Electronics, Vilnius University, Saulėtekio 9, LT-10222 Vilnius, Lithuania*
E-mail: audrius.dubietis@ff.vu.lt
[b] *University of Tartu, Institute of Physics, Riia 142, EE-51014 Tartu, Estonia*
[c] *Dipartimento di Fisica Università dell'Insubria, via Vallegio 11, IT-22100 Como, Italy*

Received 19 June 2007; revised 5 October 2007; accepted 21 November 2007

We report on highly efficient four-wave optical parametric amplification transparent bulk Kerr medium (water) under high intensity elliptical beam pumping. Energy conversion from pump to parametric waves as high as 25% is obtained owing to the achievement of 1-dimensional spatial soliton regime in noncollinear phase matching configuration, and hence guaranteeing high intensity over a large interaction length, high beam quality, and excellent operational characteristics.

Keywords: self-focusing, solitons, optical parametric amplification, four-wave mixing

PACS: 42.65.Jx, 42.65.Tg, 42.65.Yj

1. Introduction

Optical parametric amplification via three-wave interaction in non-centrosymmetric materials (birefringent crystals) is nowadays a well established technique, used for producing powerful ultrashort light pulses tunable across wide spectral range [1, 2, 3]. Optical parametric devices encompass a broad class of coherent light sources, termed multicolor lasers, which have become real workhorses in modern scientific laboratories worldwide [4, 5]. In general, parametric frequency conversion is possible in any other media, would it be solid state, liquid or gas. However, in the absence of birefringence, wave mixing processes are governed by higher order nonlinearities. In isotropic media, the lowest-order supported interaction is the four-wave mixing (FWM) driven by the third-order (cubic) susceptibility χ^3, and is much less efficient than the three-wave mixing in birefringent media owing to smaller nonlinear response. The discovery of FWM-driven optical parametric amplification dates back to the dawn of nonlinear optics [6], but most of the following studies have been directed to generation of broadband parametric radiation (supercontinuum) driven by phase-matched FWM processes in resonant and non-resonant media [7–9], see also Refs. [10, 11] for a comprehensive review on the topics. This approach is still in place today offering many possibilities for accurate measurements in spectroscopy and metrology, fibre optics, high-band telecommunications, imaging techniques, and in many other fields of modern science [12].

Despite of exciting progress in white light generation by means of FWM, four-wave parametric amplifiers are much less studied. In order to achieve efficient four-wave parametric amplification, two fundamental conditions must be fulfilled: (i) phase matching, enabling energy and momentum conservation, and (ii) good spatial overlap preserving high intensity over long beam path. In real experimental settings the above requirements get in conflict because of competing high peak power-induced effects – stimulated Raman scattering, self-focusing, self- and cross-phase modulation, and eventual optical breakdown, simultaneously occurring at nearly the same intensity threshold [13]. These factors severely limit the conversion efficiency in four-wave parametric amplification, which thus typically does not exceed several percent and is nowhere near to that compared with numbers achievable in

* The report presented at the 37th Lithuanian National Physics Conference, 11–13 June 2007, Vilnius, Lithuania.

ISSN 1648-8504

conventional χ^2-based parametric devices. Moreover, linear phase matching condition in isotropic media imposes a noncollinear interaction geometry, thus leading either to severe reduction of the interaction length or to a large phase mismatch if collinear interaction is considered. Indeed, this inconsistency is well illustrated by few recent experiments, where four-wave parametric interactions in BK7 glass and gasses (argon and air) have been studied. In the first experiment non-collinear phase-matched frequency mixing of two intense femtosecond pulses has been demonstrated in a thin BK7 glass plate under tight focusing condition, and parametric pulse energy has been limited to few μJ only due to onset of material optical damage [14]. A different approach exploited a long interaction path in a single gas filament [15]. The results outlined high beam quality but low (i. e. $\simeq 10^{-3}$) energy conversion from the pump to the generated waves despite large pump energy (1 mJ), since the collinear interaction geometry did not took an advantage of linear phase matching.

More recently, some of the present authors have reported on highly efficient performance of seeded, water-based four-wave optical parametric amplifier (FWOPA) [16]. The ultimate performance (25% energy conversion from pump to parametric waves) was achieved thanks to the discovery of a one-dimensional spatial soliton interaction regime, which successfully combined phase matching condition and high intensity over a long beam path. In this paper we provide an extended set of FWOPA characteristics, which include phase matching considerations, spatial, temporal, and spectral properties, energy conversion, and wavelength tunability.

2. Experimental set-up and phase matching considerations

In the experiment we used a Nd : glass laser system (Twinkle, Light Conversion Ltd.), which delivered frequency-doubled 1 ps, 4 mJ pulses at 527 nm at 10 Hz repetition rate. The experimental set-up schematically is depicted in Fig. 1. The laser output after frequency doubling in 11 mm long type I KDP crystal (SHG) was split by means of a beam splitter (BS) into two parts. The first portion of the laser radiation was spatially filtered and made variable in energy from 0 to 90 μJ by a combination of a $\lambda/2$ plate and thin-film polarizer (labelled as ATT) and then utilized as a pump for the FWOPA. The second portion pumped a frequency-doubled optical parametric generator (Topas, Light Conversion Ltd.), which delivered 0.7 ps pulses with wavelength tunable across the visible spectrum. After spatial filtering and suitable attenuation, selected signal pulse at wavelength $\lambda_s = 570$ nm and energy of 100 nJ was used to seed the FWOPA. The time delay between the pump and seed signal pulses was matched by means of a mechanical delay line.

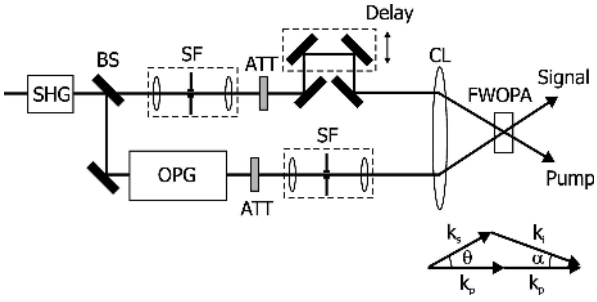

Fig. 1. Experimental set-up. SHG is the second harmonic generator, BS is the beam splitter, OPG is the optical parametric generator, ATT is the attenuator, SF is the spatial filter consisting of two lenses and a pinhole, CL is the cylindrical lens. Inset shows the phase matching geometry.

Co-polarized pump and signal beams were focused into a water cell of adjustable length using a cylindrical lens (CL) of $f_x = +500$ mm, $f_y = \infty$, which yielded beam dimensions of 1.2 mm $\times$ 130 μm at the input face of the cell, as shown in Fig. 2(b). The two beams were crossed in the plane containing the long axes of the ellipses in order to ensure good spatial overlap along entire cell length. The angle between pump and signal beams was adjusted for largest energy conversion finding an optimum phase matching. The phase-matching condition (see the inset of Fig. 1) is a vector equation: $2\mathbf{k}_\mathrm{p} = \mathbf{k}_\mathrm{s} + \mathbf{k}_\mathrm{i}$, which, projected in transverse and longitudinal directions with respect to the pump pulse reads as

$$2k_\mathrm{p} = k_\mathrm{s}\cos\theta + k_\mathrm{i}\cos\alpha\,,$$

$$k_\mathrm{s}\sin\theta = k_\mathrm{i}\sin\alpha\,, \qquad (1)$$

where $k(\omega) = n(\omega)\,\omega/c$ is the wave number, θ and α denote the angles of the signal and idler beams with respect to the pump beam axis, and indexes p, s, i stand for the pump, signal, and idler waves, respectively. After simple algebra, one finds the phase matching angle between the pump and signal beams:

$$\cos\theta = \frac{(2k_\mathrm{p})^2 + (k_\mathrm{s})^2 - (k_\mathrm{i})^2}{4k_\mathrm{s}k_\mathrm{p}}\,. \qquad (2)$$

For the chosen wavelengths of $\lambda_\mathrm{p} = 527$ nm and $\lambda_\mathrm{s} = 570$ nm, and taking into account the dispersion

relation for water [17], the calculated external (in air) phase matching angle is $\theta = 1.33°$.

3. Generation of parametric solitons

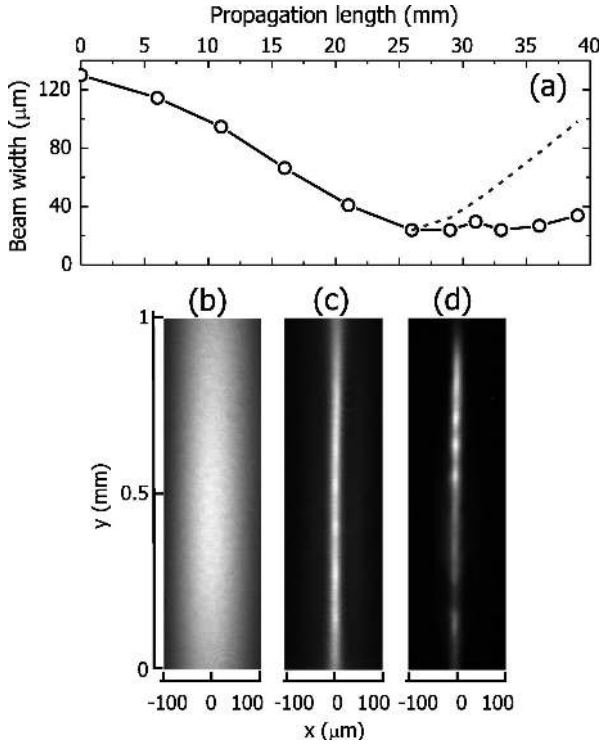

Fig. 2. (a) FWHM width of the pump beam versus propagation. Near field intensity profiles of (b) input pump beam; (c) pump and (d) signal beams at the output face of the 40 mm long water cell. The diffraction of the Gaussian beam is depicted by a dashed line.

Recently it has been demonstrated that highly elliptical beams experience one-dimensional self-focusing in the short axis direction and after passing the nonlinear focus break up into an array of almost equally spaced multiple filaments [18]. The beam break-up is caused by transverse modulational instability, an universal phenomenon observed in all nonlinear media [19]. In our experimental settings maximum beam power equals to $\sim 80\, P_{\rm cr}$ and the beam break-up occurs at $z \approx 20$ mm. Here $P_{\rm cr} = 3.77\,\lambda^2/(8\pi n n_2) = 1.15$ MW is the critical power for self focusing, with $\lambda = 527$ nm being the wavelength, $n = 1.33$ the linear and $n_2 = 2.7{\cdot}10^{-16}$ cm^2/W the nonlinear refractive indexes of water, respectively. However, the injection of a weak seed signal at the phase matching angle leads to quenching of filament formation and beam break-up. In this case the pump beam contracts along its short axis direction and forms a uniform light stripe of 24 μm short-axis FWHM diameter, which propagates over $\sim$15 mm distance inside the water cell without apparent diffraction [see Fig. 2(a)], as measured by imaging the output face of a variable length water cuvette onto a CCD camera (COHU-6612 with Spiricon Inc. frame grabber). Note that this distance is $\sim$4.5 times larger than the diffraction length for a Gaussian beam of the same diameter.

The signal and idler modes exhibit diffraction-free propagation as well, being trapped within a gain channel created by intense pump beam and thus providing an ideal condition for efficient parametric amplification to take place. Examples of near-field images of pump and signal modes at the exit of 40 mm long water cell are depicted in Fig. 2 (c) and (d), respectively. The overall observation suggests the formation of stable multicolor parametric one-dimensional spatial solitons. In our settings the pump beam break-up threshold is notably increased due to strong phase-matched four-wave parametric interaction. Here off-axis propagating signal and idler modes act as a damping mechanism that suppresses any local spike that forms in the pump beam. The soliton regime is sustained with pump beam energy as high as 90 μJ, and with seed pulse energy as low as 10 nJ. We note that in bulk Kerr medium, stable one-dimensional spatial solitons have been observed just on several occasions and just under specific operating conditions, where transverse instabilities have been suppressed by self-induced waveguiding through interference [20], periodic azimuthal modulation of ring beams [21], and by making the beams partially incoherent [22]. We also mention that present situation is different from the multicolor soliton regime in planar waveguides, in space of reduced dimensionality [23, 24].

4. FWOPA operation

Figure 3 shows measured FWOPA output energy versus pump energy $E_{\rm p}$. Detectable amplification of the seed signal starts at pump energy as low as 10 μJ and saturates at $E_{\rm p} = 60$ μJ. At gain saturation the overall energy conversion to parametric waves (including cascaded components) is as high as 25%. The result also outlines a signal amplification factor of $\approx$100, with pump-to-signal energy conversion of 15% at $E_{\rm p} = 60$ μJ. We underline the two relevant features observed in FWOPA operation: the first one considers a strong cascading, that is justified by the emergence of a comb of upshifted and downshifted frequency components (shown in the far-field photograph in Fig. 4(a)), while the second one points to apparent energy unbalance

in the signal and idler waves, the idler wave at $\lambda_{\rm i} =$ 490 nm being ∼3.5 times weaker. In what follows, we interpret the observed features as the nontrivial impact of the phase matching and absorption on the multi-step four-wave parametric processes.

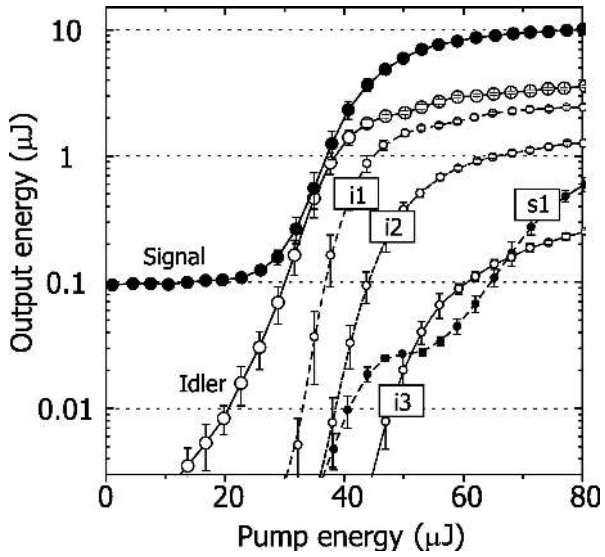

Fig. 3. Energy of signal (full circles and solid curve), idler (open circles and solid curve), and cascaded components (dashed curves) versus pump energy $E_{\rm p}$.

The cascaded modes are generated through the multi-step FWM processes: $\mathbf{k}_{\rm s1} = 2\mathbf{k}_{\rm s} - \mathbf{k}_{\rm p}, \mathbf{k}_{\rm i1} = 2\mathbf{k}_{\rm i} - \mathbf{k}_{\rm p}, \mathbf{k}_{\rm i2} = 2\mathbf{k}_{\rm i1} - \mathbf{k}_{\rm i}$, etc. [14], here signal and idler and afterwards the cascaded components serving as a pump for new FWM processes. The frequencies of the cascaded components differ by the constant frequency shift $\Delta\omega = \omega_{\rm p} - \omega_{\rm s}$ and can be expressed by the following equations:

$$\omega_{{\rm s}n} = (n+1)\omega_{\rm s} - n\omega_{\rm p}\,,$$

$$\omega_{{\rm i}n} = (n+1)\omega_{\rm i} - n\omega_{\rm p}\,, \qquad (3)$$

where subscripts in and sn denote upshifted (idler) and downshifted (signal) components, termed as cascaded idlers and signals, respectively, and n stands for the cascading order. Figure 4(b) plots experimentally measured angles of the pump, signal, idler, and cascaded modes superimposed on the calculated phase matching curve. It is interesting to note that the cascading is favoured towards the blue side of the spectrum, with the components detected at $\lambda_{\rm i1} = 458$ nm, $\lambda_{\rm i2} = 430$ nm, $\lambda_{\rm i3} = 405$ nm, and $\lambda_{\rm i4} = 383$ nm, whereas fewer red-shifted components measured at $\lambda_{\rm s1} = 621$ nm and $\lambda_{\rm s2} = 681$ nm. In order to explain this observation, we recall that water absorption increases continuously from the blue toward the near infrared, with the maximum transparency at 417 nm [25]. The unequal number of upshifted and downshifted modes can be explained by an impact of absorption on the gain profile. Absorption of one of the interacting (coupled) waves is expected to reduce the gain of the particular four-wave parametric process as a whole, and unevenly modifies the gain for the cascaded processes. Therefore, an appreciable gain occurs rather for the processes responsible of producing frequency upshifted components than for those producing frequency downshifted ones. Moreover, the phase matching condition (1), if applied to the cascaded modes occurring at different angles with respect to the pump beam (these are shown in Fig. 4(b), being determined by the injection angle of the seed signal), suggests small phase mismatch for generation of the blue-shifted cascaded modes. In contrast, phase mismatch is considerably higher toward the red-shifted frequencies, as shown in Fig. 4(c). We also note that the possibility of interactions of type $\mathbf{k}_{\rm i1} = 2\mathbf{k}_{\rm p} - \mathbf{k}_{\rm s1}$ is generally ruled out because the cascaded components do not appear in pairs (first cascaded signal with first cascaded idler, etc.) as evident from energy measurements presented in Fig. 3.

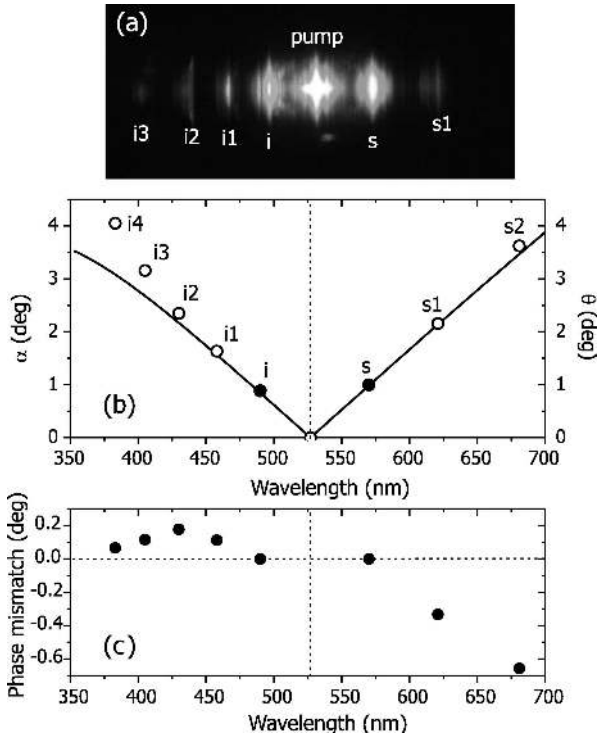

Fig. 4. (a) Screen shot of the FWOPA output. (b) Phase matching curve (solid line) and measured angles of the signal, idler, and cascaded modes with respect to the pump beam (circles). (c) Phase mismatch angles.

For what concerns the observed energy unbalance, we note that the amount of energy, originally generated in the idler wave through the primary parametric process (amplification of the seed signal) is strictly governed by the Manley–Rowe equation, which yields an equal number of photons created in the signal and idler waves via parametric interaction. Indeed, it was confirmed by the analysis in terms of photon numbers of cascaded four-wave interactions in optical fibres [26] and more recently in the case of noncollinear four-wave optical parametric amplification [16]. It is worth noting that the cascading not only involves the redistribution of the energy between the signal (idler) wave and its cascaded counterparts, but also the transfer of some amount of energy back to the pump wave (back conversion). Since the gain for particular cascaded process varies with frequency due to absorption, less cascading is observed toward larger absorption and concomitantly less energy (or photon number) is back-converted to the pump. This fact was verified by launching the signal with wavelength shorter that that of the pump ($\lambda_{\rm s} = 490$ nm), with obtaining stronger blue-shifted cascading, but the amplified signal energy being 3.5 times lower that the generated idler wave at $\lambda_{\rm i} = 570$ nm.

In our settings the cascaded components comprise 20% of the total output energy and contribute to less than 5% of the overall energy conversion. The number as well as the energy of the cascaded components, which in most cases is undesirable energy loss, can be minimized with tuning the seed signal wavelength farther from the pump. An interesting situation occurs if the FWOPA is seeded at the Raman line. In this case, it is expected that the Raman gain, which is non-parametric process, and therefore does not require phase matching, might contribute to the parametric amplification process. Indeed, choosing the seed signal wavelength at 637 nm, which is exactly the Raman shift for water, we have measured a notable enhancement of the signal gain (up to 450) with just 40 nJ input signal.

5. Spectral and autocorrelation measurements

In this section we provide characterization of FWOPA operation in spectral and temporal domain. Spectral measurements were performed using a fibre spectrometer (QE65000, Ocean Optics). Figure 5 compares single shot spectra of the seed and amplified signal pulses. The spectral shape of the amplified signal remains basically unchanged and exhibits just negligible spectral broadening from 82 to 98 cm^{-1}. The estimated time–bandwidth product of the amplified signal with account for measured pulse duration ($\tau_{\rm p} = 0.5$ ps) is $\tau_{\rm p} \cdot \Delta\nu = 1.47$ and remains close to that of the input seed pulse ($\tau_{\rm p} \cdot \Delta\nu = 1.72$). We have also measured the spectral gain profile of the FWOPA, by scanning the seed wavelength while keeping the pump and signal intersection angle fixed (data is not shown). The measured FWHM of the gain profile is 3 nm, that in fact can be expected from the steepness of the phase matching curve.

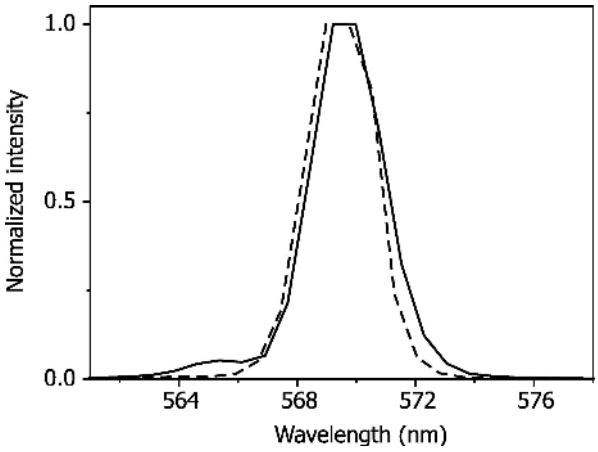

Fig. 5. Spectra of seed (dashed curve) and amplified (solid curve) signal pulses.

Autocorrelation measurements were performed using an imaging scanning autocorrelator, which selected just the central portion of the elliptical beam and imaged it onto 100 μm thick nonlinear crystal (BBO). A set of results is plotted in Fig. 6. Panels (a) and (d) show the autocorrelation traces for input pump (1 ps) and seed signal (0.7 ps) pulses, respectively. Panels (b) and (e) represent autocorrelation functions at the output of 40 mm long water cell of the undepleted pump pulse and the amplified signal, respectively, measured with $E_{\rm p} = 60$ μJ, where gain saturation occurs. Although during the propagation both pump and signal pulses experience some transient shortening associated with soliton formation regime (data not shown), the amplified signal pulse at the FWOPA output exhibits a clean Gaussian profile with good shot-to-shot reproducibility (note small error bars). With $E_{\rm p} = 80$ μJ, pump pulse alone (with no seed) breaks up into an array of multiple filaments, which in turn prompts pulse splitting in time into two sub-pulses, as shown by 3-peak autocorrelation function in Fig. 6(c), appearance of conical emission, and, finally, formation of the X-waves [27]. By contrast, temporal splitting of the pump pulse is quenched when a seed signal is launched, and a clean amplified signal with a Gaussian profile is measured,

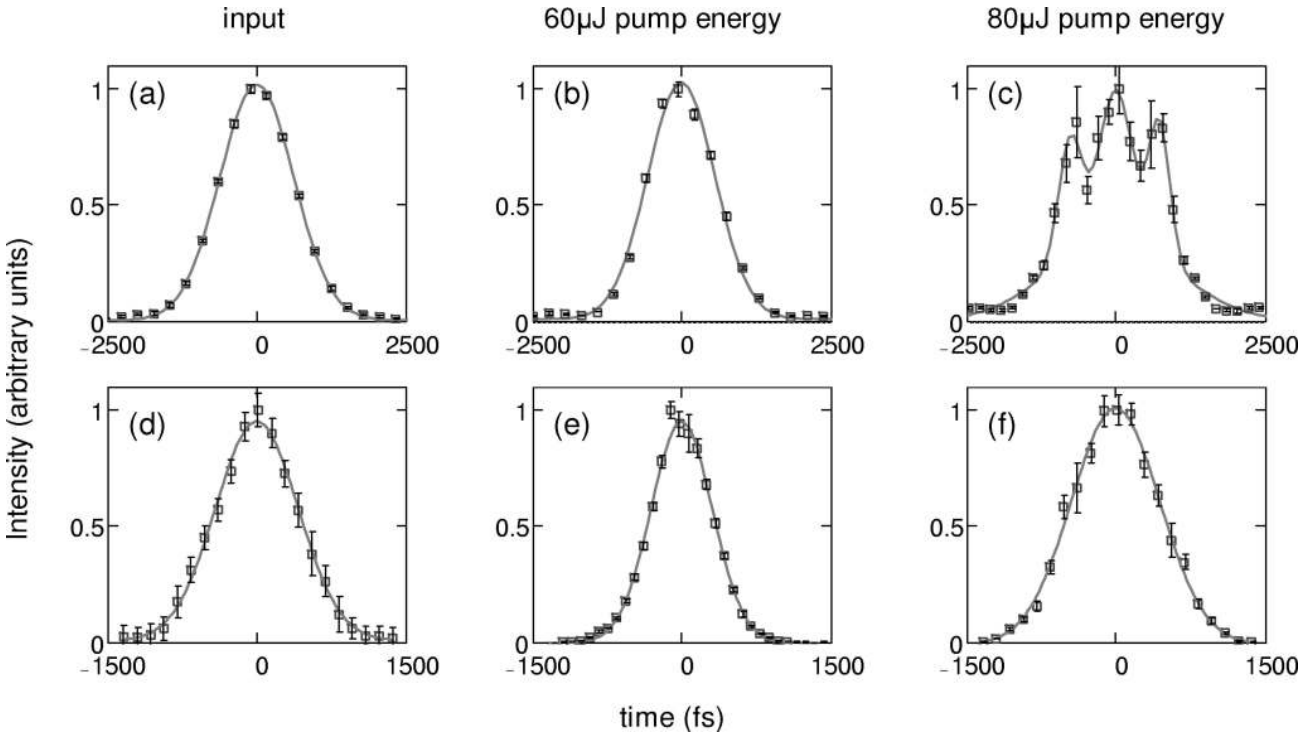

Fig. 6. Normalized autocorrelation functions of pump (a–c) and signal (d–f) pulses. Open squares stand for measured data, while solid curves show the Gaussian fit. See text for details.

see Fig. 6(f). However, in gain saturation regime, the amplified pulse is measured to be slightly longer, that is due to strong energy back-conversion to the pump and cascaded pulses, as discussed in previous section.

6. Conclusions

In conclusion, we have demonstrated an operating condition for highly efficient four-wave parametric amplification in a bulk isotropic and transparent medium with Kerr nonlinearity (water) in the visible spectral range. With overall figure of 25% energy conversion from pump to parametric waves, FWOPA is simple, inexpensive, and ready to use frequency converter with high operational characteristics. An excellent performance has been achieved by the use of cylindrical focusing, which allows simultaneously fulfilment of noncollinear phase matching condition and good spatial overlap between the interacting beams over long path length. Under these settings, efficient four-wave interaction quenched the transverse beam break-up of the intense pump and permitted the achievement of 1-dimensional spatial soliton regime in bulk medium, never observed before to the best of our knowledge. Differently from the tight focusing configuration, our set-up operates far from the threshold of optical breakdown, and differently from the filament-mediated four-wave parametric amplification, the spatial soliton regime is not limited in one transverse dimension (along the long axis of an ellipse), so the present setup can be easily scaled in size and energy. The soliton regime could be easily adopted to virtually all transparent media, including solid-state and gaseous, and for a variety of wavelengths, where conventional phase matching techniques based on material birefringence are not applicable. And finally, our finding of quenching spontaneous break-up and filamentation of intense laser beams by launching a weak seed signal opens new route towards generation of fully controllable propagation of multifilamentary structures.

Acknowledgements

H. V. and P. P. acknowledge the support from Sixth EU Framework Programme Contract No. MEST-CF-2004-008048 (ATLAS), P. D.T. acknowledges the support from Marie Curie Chair project STELLA (`www.vino-stella.eu`), Contract No. MEXC-CT-2005-025710.

References

[1] M.H. Dunn and M. Ebrahimzadeh, Parametric generation of tunable light from continous-wave to femtosec-

ond pulses, Science **286**, 1513–1517 (1999).
[2] G. Cerullo and S. De Silvestri, Ultrafast optical parametric amplifiers, Rev. Sci. Instrum. **74**, 1–18 (2003).
[3] A. Dubietis, R. Butkus, and A. Piskarskas, Trends in chirped pulse optical parametric amplification, IEEE J. Sel. Topics Quantum Electron. **12**, 163–172 (2006).
[4] W. Sibbett and M. Padgett, Multicolor lasers, Physics World **6**, 36–40 1993.
[5] A. Piskarskas, Optical parametric generators: Tunable, powerful, ultrafast, Opt. Photon. News **7**, 25–28 (1997).
[6] R.L. Carman, R.Y. Chiao, and P.L. Kelley, Observation of degenerate stimulated four-photon interaction and four-wave parametric amplification, Phys. Rev. Lett. **17**, 1281–1284 (1966).
[7] R.R. Alfano and S.L. Shapiro, Emission in the region 4000 to 7000 Å via four-photon coupling in glass, Phys. Rev. Lett. **24**, 584–587 (1970).
[8] A. Penzkofer, A. Laubereau, and W. Kaiser, Stimulated short-wave radiation due to single-frequency resonances of $\chi^{(3)}$, Phys. Rev. Lett. **31**, 863–866 (1973).
[9] M. Wittmann and A. Penzkofer, Spectral superbroadening of femtosecond laser pulses, Opt. Commun. **126**, 308–317 (1996).
[10] R.R. Alfano, *The Supercontinuum Laser Source* (Springer, New York, 2006).
[11] G.P. Agrawal, *Nonlinear Fiber Optics* (Academic Press, London, 1989).
[12] R.R. Alfano, The ultimate white light, Sci. Am. **295**, 86–93 (2006).
[13] A. Penzkofer and H.J. Lehmeier, Theoretical investigation of noncollinear phase-matched parametric four-photon amplification of ultrashort light pulses in isotropic media, Opt. Quantum Electron. **25**, 815–844 (1993).
[14] H. Crespo, J.T. Mendonça, and A. Dos Santos, Cascaded highly nondegenerate four-wave-mixing phenomenon in transparent isotropic condensed media, Opt. Lett. **25**, 829–831 (2000).
[15] F. Théberge, N. Aközbek, W. Liu, A. Becker, and S.L. Chin, Tunable ultrashort laser pulses generated through filamentation in gases, Phys. Rev. Lett. **97**, 023904 (2006).
[16] A. Dubietis, G. Tamošauskas, P. Polesana, G. Valiulis, H. Valtna, D. Faccio, P. Di Trapani and A. Piskarskas, Highly efficient four-wave parametric amplification in transparent bulk Kerr medium, Opt. Express **15**, 11126–11132 (2007).
[17] A.G. Van Engen, S.A. Diddams, and T.S. Clement, Dispersion measurements of water with white-light interferometry, Appl. Opt. **37**, 5679–5686 (1998).
[18] A. Dubietis, E. Kučinskas, and G. Tamošauskas, Formation of periodic multifilamentary structures by use of highly elliptical light beams, Lithuanian J. Phys. **47**, 27–30 (2007).
[19] Y.S. Kivshar and D. Pelinovsky, Self-focusing and transverse instabilities of solitary waves, Phys. Rep. **331**, 117–195 (2000).
[20] A. Barthelemy, S. Maneuf, and C. Froehly, Propagation soliton et auto-confinement de faisceaux laser par non linearité optique de Kerr, Opt. Commun. **55**, 201–206 (1985).
[21] M. Soljačić, S. Sears, and M. Segev, Self-trapping of "Necklace" beams in self-focusing Kerr media, Phys. Rev. Lett. **81**, 4851–4854 (1998).
[22] C. Anastassiou, M. Soljačić, M. Segev, E.D. Eugenieva, D.N. Cristodoulides, D. Kip, Z.H. Musslimani, and J.P. Torres, Eliminating the transverse instabilities of Kerr solitons, Phys. Rev. Lett. **85**, 4888–4891 (2000).
[23] P.B. Lundquist, D.R. Andersen, and Y.S. Kivshar, Multicolor solitons due to four-wave mixing, Phys. Rev. E **57**, 3551–3555 (1998).
[24] G. Fanjoux, J. Michaud, M. Delqué, H. Mailotte, and T. Sylvestre, Generation of multicolor Kerr solitons by cross-phase modulation, four-wave mixing, and stimulated Raman scattering, Opt. Lett. **31**, 3480–3482 (2006).
[25] R.M. Pope and E.S. Fry, Absorption spectrum (380–700 nm) of pure water. II. Integrating cavity measurements, Appl. Opt. **36**, 8710–8723 (1997).
[26] D.L. Hart, A. Judy, T.A.B. Kennedy, R. Roy, and K. Stoev, Conservation law for multiple four-wave-mixing processes in a nonlinear optical medium, Phys. Rev. A **50**, 1807–1814 (1994).
[27] A. Couairon, E. Gaižauskas, D. Faccio, A. Dubietis, and P. Di Trapani, Nonlinear X-wave formation by femtosecond filamentation in Kerr media, Phys. Rev. E **73**, 016608 (2006).

EFEKTYVUS KETURBANGIS PARAMETRINIS ŠVIESOS STIPRINIMAS IR ERDVINIŲ SOLITONŲ GENERACIJA SKAIDRIOJE IZOTROPINĖJE TERPĖJE SU KERR'O NETIESIŠKUMU

H. Valtna [a,b], A. Dubietis [a], G. Tamošauskas [a], P. Polesana [a,c], J. Galinis [a], D. Majus [a], G. Valiulis [a], D. Faccio [c], P. Di Trapani [a], A. Piskarskas [a]

[a] *Vilniaus universiteto Fizikos fakultetas, Vilnius, Lietuva*
[b] *Tartu universitetas, Tartu, Estija*
[c] *Insubrijos universitetas, Como, Italija*

Santrauka

Pademonstruotas didelio efektyvumo keturbangis parametrinis šviesos stiprinimas skaidrioje izotropinėje terpėje su Kerro netiesiškumu (vandenyje), kaupinant eliptiniais šviesos pluoštais. Gautas energinis keitimas iš kaupinimo į parametrines bangas yra 25%. Tokios sąveikos metu realizuotas vienmačių erdvinių solitonų režimas, įgalinęs užtikrinti nekolinearų fazinį sinchronizmą, didelį kaupinimo intensyvumą dideliame sąveikos ilgyje, o taip pat aukštas spinduliuotės laikines ir erdvines charakteristikas.